

# ChemComm

Accepted Manuscript



This is an *Accepted Manuscript*, which has been through the Royal Society of Chemistry peer review process and has been accepted for publication.

*Accepted Manuscripts* are published online shortly after acceptance, before technical editing, formatting and proof reading. Using this free service, authors can make their results available to the community, in citable form, before we publish the edited article. We will replace this *Accepted Manuscript* with the edited and formatted *Advance Article* as soon as it is available.

You can find more information about *Accepted Manuscripts* in the [Information for Authors](#).

Please note that technical editing may introduce minor changes to the text and/or graphics, which may alter content. The journal's standard [Terms & Conditions](#) and the [Ethical guidelines](#) still apply. In no event shall the Royal Society of Chemistry be held responsible for any errors or omissions in this *Accepted Manuscript* or any consequences arising from the use of any information it contains.

## COMMUNICATION

# Coordination reaction between tetraphenylporphyrin and nickel on a TiO<sub>2</sub>(110) surface†

Cite this: DOI: 10.1039/x0xx00000x

Cici Wang,<sup>a</sup> Qitang Fan,<sup>a</sup> Shanwei Hu,<sup>a</sup> Huanxin Ju,<sup>a</sup> Xuefei Feng,<sup>a</sup> Yong Han,<sup>a</sup> Haibin Pan,<sup>a</sup> Junfa Zhu,<sup>\*a</sup> and J. Michael Gottfried<sup>\*b</sup>Received 00th January 2014,  
Accepted 00th January 2014

DOI: 10.1039/x0xx00000x

www.rsc.org/

**In-situ metalation of tetraphenylporphyrin (2HTPP) (sub)monolayers with Ni on a TiO<sub>2</sub>(110) surface to nickel(II)-tetraphenylporphyrin (NiTPP) depends on temperature and order of deposition, and affects conformation and bonding geometry of the porphyrin.**

Metalloporphyrins have high potential for applications as building blocks for the design of supramolecular architectures,<sup>1</sup> in gas sensors,<sup>2</sup> spintronics<sup>3</sup> and as catalysts<sup>4</sup>. Recently, it has been shown that metalloporphyrins can be synthesized under ultra-high vacuum (UHV) conditions by a redox reaction between adsorbed metal-free porphyrins (e.g., tetraphenylporphyrin, 2HTPP) and metal atoms. This metalation process works with post- or pre-deposited metal atoms<sup>5,6</sup> or intrinsic substrate atoms<sup>7</sup> on well-defined metal surfaces. However, to our knowledge, porphyrin metalation on oxide surfaces has not been observed before, although metalloporphyrins on oxides are interesting as catalysts: CoTPP supported on TiO<sub>2</sub> effectively catalyzes the reduction of NO<sub>x</sub> with H<sub>2</sub> or CO<sup>8</sup> and the photocatalytic degradation of dyes.<sup>9</sup>

We selected rutile TiO<sub>2</sub>(110) as the oxide substrate to study the metalation of 2HTPP with Ni, because rutile TiO<sub>2</sub>(110)-1×1 can be prepared with large atomically flat terraces. This surface thus offers an effective platform for adsorbate characterization via surface science techniques, such as X-ray photoelectron spectroscopy (XPS) and scanning tunnelling microscopy (STM). So far, only a few studies exist about adsorption of porphyrinoids on TiO<sub>2</sub>(110). Rienzo et al. found a strong interaction of zinc-protoporphyrin with TiO<sub>2</sub>, such that the Zn atom is pulled out of the molecule.<sup>10</sup> In another study, a highly localized interaction between zinc(II) etioporphyrin molecules and oxygen vacancies on TiO<sub>2</sub>(110) was found by lateral manipulation of the molecule with an STM tip.<sup>11</sup> In this work, XPS and STM were employed for a quantitative study of the metalation of (sub)monolayer coverages of 2HTPP with Ni atoms on TiO<sub>2</sub>(110)-1×1, revealing interesting similarities and differences to porphyrin metalation on metal surfaces.

Figure 1a shows the N 1s XPS spectrum of a monolayer of 2HTPP on TiO<sub>2</sub>(110)-1×1. The two components with binding energies of 400.1 and 398.2 eV are assigned to pyrrolic (-NH-) and iminic nitrogen (=N-), respectively, in agreement with previous work.<sup>5b,5g</sup>

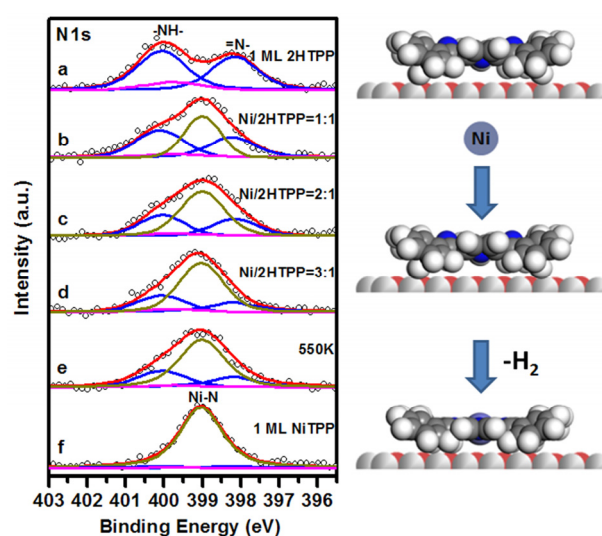


Figure 1. N 1s XPS spectra of (a) a monolayer of 2HTPP on TiO<sub>2</sub>(110)-1×1, (b-d) after incremental deposition of Ni with the indicated Ni/2HTPP ratios onto sample (a), (e) after heating sample (d) to 550 K, and (f) N 1s XPS spectrum of a monolayer of NiTPP on TiO<sub>2</sub>(110) for comparison. The following line colours are used for the fitting curves: blue = 2HTPP, dark yellow = NiTPP, magenta = additional satellite peak to account for shakeup processes (ESI†), and red = envelope.

Post-deposition of a stoichiometric amount of nickel (i.e., one Ni atom per 2HTPP molecule) onto the 2HTPP monolayer at 300 K leads to substantial changes: the two 2HTPP related N 1s peaks lose intensity, while a new peak appears at 399.0 eV, as shown by Figure 1b (dark yellow line). The binding energy (BE) of this new peak is identical to the reference spectrum in Figure 1f, obtained from a monolayer of NiTPP that was directly vapour-deposited onto the TiO<sub>2</sub>(110) surface. Therefore, this new peak at 399.0 eV is attributed to N atoms in NiTPP<sup>6a</sup> formed by reaction between 2HTPP and Ni following the equation  $2\text{HTPP} + \text{Ni} \rightarrow \text{NiTPP} + \text{H}_2$ . The corresponding oxidation of Ni(0) to Ni(II) can be seen in the Ni 2p<sub>3/2</sub> XPS spectra in Figure S1 of the ESI†. By comparing the integrated areas for all components in the N 1s XPS spectrum, the yield of NiTPP was determined to be (35 ± 5)% of the initial 2HTPP, which is a lower yield than previously found for porphyrin metalation on metal surfaces.<sup>5b, 6a</sup> Further increasing the amount of Ni to

Ni/2HTPP ratios of 2:1 and 3:1 leads to further formation of NiTPP, as evidenced by the increased intensity of the NiTPP related N 1s component in Figure 1c and 1d. However, even with a Ni/2HTPP ratio of 3:1 only ( $60 \pm 5\%$ ) of 2HTPP are converted to NiTPP (*cf.* Table S1, ESI<sup>†</sup>), i.e., the metalation degree is not proportional to the amount of Ni. This is attributed to the increasing probability that adsorbing Ni atoms add to Ni clusters instead of reacting with 2HTPP (*cf.* Figure S1, ESI<sup>†</sup>). Heating the sample in Figure 1d to 550 K (Figure 1e) does not increase the metalation ratio.

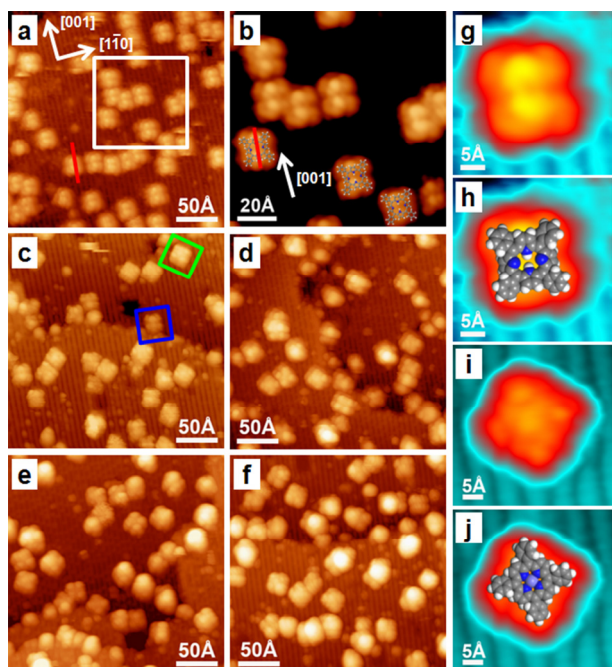


Figure 2. Constant-current STM images (a) after deposition of  $\sim 0.1$  ML 2HTPP onto  $\text{TiO}_2(110)\text{-}1\times 1$ . The red line represents a molecular mirror plane. (b) Enlarged image of the white square indicated in (a) overlaid with molecular models. (c-e) STM images after incremental deposition of Ni onto the sample with Ni/2HTPP ratios of 1:1, 2:1, and 3:1. In image (c), two types of molecules are labelled by blue and green squares. (f) After heating sample (e) to 550 K. (g, i) High resolution STM images of two types of single molecules and (h, j) images superimposed with corresponding molecular models. Tunnelling parameters: (a)  $I = 0.04$  nA; (b)  $I = 0.03$  nA; (c)  $I = 0.04$  nA; (d)  $I = 0.03$  nA; (e)  $I = 0.06$  nA; (f)  $I = 0.03$  nA; (g, h)  $I = 0.04$  nA; (i, j)  $I = 0.03$  nA. All sample bias voltages are  $-2.2$  V.

The corresponding STM experiments were conducted with a 2HTPP submonolayer on  $\text{TiO}_2(110)$ . Figure 2a shows the overview STM image after deposition of  $\sim 0.1$  ML 2HTPP onto  $\text{TiO}_2(110)$  at 300 K. According to XPS, these adsorbates are intact 2HTPP. Instead of the 4-fold symmetry of free 2HTPP, the adsorbed molecules show a 2-fold symmetry, which is typical for the saddle-shape conformation that tetraarylporphyrins are known to adopt on metal surfaces.<sup>12</sup> The molecules are disordered and do not self-assemble in close-packed islands. This behaviour is typical for 2HTPP on strongly interacting surfaces such as  $\text{Cu}(111)$ , where the iminic N atoms form bonds to substrate atoms. Another similarity to 2HTPP on  $\text{Cu}(111)$  is the alignment of the molecular mirror plane with high-symmetry directions of the substrate.<sup>13</sup> Here, on  $\text{TiO}_2(110)$ , the molecular mirror plane through the two protrusions is nearly parallel to the [001] direction, indicating a rotational barrier posed by strong adsorbate-substrate interaction as previously observed for 2HTPP on  $\text{Cu}(111)$ .<sup>13a,7d</sup> Figure 2g shows an STM image with submolecular resolution of a single 2HTPP molecule (overlaid with a molecular model in Figure 2h) with the substrate resolved. The bright rows

along the [001] direction correspond to rows of five-fold coordinated  $\text{Ti}^{4+}$  ions.<sup>14</sup> The centres of the 2HTPP molecules lie in the dark rows, which correspond to the bridging oxygen rows.<sup>14b</sup> Thus we tentatively propose that the H atoms of the two pyrrolic groups ( $-\text{NH}-$ ) are pointing downwards forming hydrogen bonds with the surface bridging oxygen atoms. The N 1s XPS core level shifts support this interpretation: On  $\text{Cu}(111)$ , with which 2HTPP also interacts strongly, but in this case through its iminic N atoms ( $=\text{N}-$ ), the separation between the two N 1s components is only 1.5 eV,<sup>13a</sup> in contrast to the 1.9 eV found here for 2HTPP on  $\text{TiO}_2(110)$  (Figure 1a). On  $\text{Cu}(111)$ , the small peak separation results from a shift of the iminic peak to higher BE caused by electron donation from the iminic N to the Cu surface.<sup>13a</sup> Despite the fact that 2HTPP also interacts strongly with  $\text{TiO}_2$ , this type of bond is apparently not formed on this surface, in agreement with the proposed H bonding through the pyrrolic groups ( $-\text{NH}-$ ).

Figure 2c shows the STM image acquired after deposition of the stoichiometric amount of Ni (i.e., one Ni atom per 2HTPP) onto the sample in Figure 2a at 300 K. Interestingly, after deposition of Ni, some of the molecules undergo a  $\sim 45^\circ$  rotation (example marked with green square) relative to 2HTPP (example marked with blue square). A magnified view of the rotated molecule in Figure 2i shows a flat conformation with four-fold symmetry, suggesting that the metalation reduces the apparent height and conformational flexibility of the porphyrin. Furthermore, statistical analysis of 24 STM images taken on the same sample as Figure 2c (*cf.* Table S1, ESI<sup>†</sup> for details) show that the proportion of rotated molecules is  $(32 \pm 8)\%$ , which agrees with the  $(35 \pm 5)\%$  fraction of NiTPP calculated from the XPS data for the stoichiometric Ni:2HTPP ratio. Thus we assign these rotated four-fold symmetric molecules to NiTPP (see the overlaid molecular model in Figure 2j) formed by metalation. Increasing the amount of deposited Ni to Ni:2HTPP ratios of 2:1 and 3:1 leads to more metalation. This again agrees with the XPS results presented above (*cf.* Table S1, ESI<sup>†</sup>). Figure 2f shows the STM image after further annealing to 550 K (*cf.* Figure 2e): the degree of metalation does not increase, which is again consistent with the XPS results in Figure 1. A likely reason for this finding is the formation of large, stable Ni clusters in combination with the known low mobility of Ni atoms on  $\text{TiO}_2(110)$ .<sup>15</sup>

As shown in Figures 3a and 3b, the apparent heights of 2HTPP (green line) and NiTPP (black line) are 6 Å and 5 Å, respectively (*cf.* Figures 3e and 3f). This height difference is mainly caused by the change from a saddle-shape conformation to a flat conformation, as schematically visualized by the molecular models in Figures 3c and 3d. Further inspection of Figures 3a and 3b reveals NiTPP (blue line) and 2HTPP (magenta line) species which carry bright protrusion. Apparent height profiles across these species are shown in Figures 3g and 3h. In both cases, the maximum apparent height is 9 Å relative to the substrate. The bright dots on the molecules are assigned to Ni atoms or small clusters sitting on-top of the porphyrin molecules, because none of these molecules with protrusions occur before Ni deposition. Similar observations have previously been made for Fe deposition onto CoTPP on  $\text{Ag}(111)$ , where the Fe atoms occupy off-center positions on the CoTPP molecules.<sup>16</sup> A single Fe atom on CoTPP increases the apparent height by almost 3 Å. Therefore, it is possible that the additional protrusions observed in our study result from single Ni atoms or clusters of monoatomic height on the porphyrin molecules. Apparently, Ni atoms (or small clusters) can occasionally even sit on unmetalated 2HTPP without metalation to occur. This can tentatively be attributed to a substantial barrier for the transition from the off-center bound Ni atom to an initial sitting-atop complex.<sup>5h</sup>



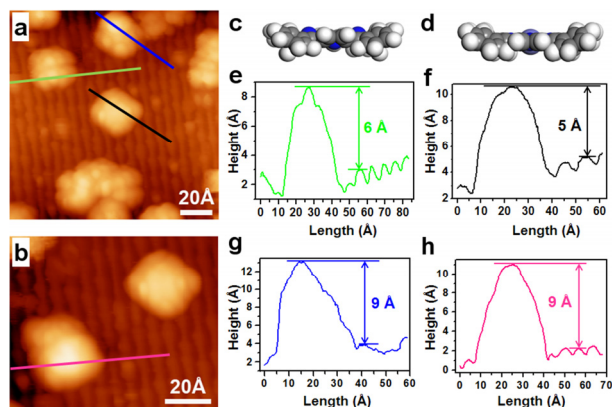


Figure 3. (a, b) Constant-current STM images after deposition of a stoichiometric amount of Ni onto 0.1 ML 2HTPP on  $\text{TiO}_2(110)-1 \times 1$  ( $\theta_{\text{Ni}} = 0.01$ , Ni:2HTPP = 1:1). Tunnelling parameters:  $U = -2.2$  V,  $I = 0.03$  nA. (c) Side view model of 2HTPP with a marked saddle-shaped conformation, where the pyrrolic nitrogen atoms are pointing downwards. (d) Side view model of NiTPP conformation with a flat macrocycle. (e-h) Apparent height profiles of the features marked with lines of corresponding colors in the STM images (a) and (b).

In the following, the order of deposition was reversed, i.e., Ni was pre-deposited onto  $\text{TiO}_2(110)$  at 300 K and then a monolayer 2HTPP was deposited. In contrast to the procedure with Ni post-deposition, the N 1s spectrum (Figure 4a) shows only 2HTPP related signals, which indicates that no metalation occurred. After annealing to 550 K, the NiTPP-related peak at 399.0 eV appears, as shown in Figure 4b, indicating the formation of NiTPP. Similar observations were made for 2HTPP/Ni/Au(111),<sup>6a</sup> where it was suggested that elevated temperatures are needed to overcome the activation barrier for the transition of the Ni atom from the surface (or from a Ni cluster) to the 2HTPP molecule and for increasing the 2D vapour pressure of Ni atoms in equilibrium with the Ni clusters. Figure 4c shows an STM image taken after deposition of submonolayer Ni ( $\theta_{\text{Ni}} = 0.01$ ) onto  $\text{TiO}_2(110)-1 \times 1$ . Ni forms non-uniform clusters that distribute randomly at both terraces and step edges. After vapor deposition of 2HTPP onto this sample (cf. Figure 4c) at 300 K, no rotated molecules (NiTPP) can be seen (cf. Figure 4d), indicating that no metalation occurred. However, after the sample was heated to 550 K, rotated four-fold symmetric molecules (example marked by green square) appear, indicating formation of NiTPP. Moreover, the fraction of NiTPP calculated by both XPS and STM is almost the same as for Ni/2HTPP/ $\text{TiO}_2(110)$  (cf. Table S1, ESI†).

Using XPS and STM, we have shown that NiTPP can be synthesized in-situ on a  $\text{TiO}_2(110)-1 \times 1$  surface from vapor-deposited Ni atoms and 2HTPP. If Ni is deposited onto (sub)monolayer 2HTPP on  $\text{TiO}_2$ , the reaction proceeds already at room temperature, while elevated temperatures are required when Ni is deposited first. The reaction from 2HTPP to NiTPP is accompanied by changes of the molecular conformation from saddle-shaped to a four-fold symmetry. These results provide a new insight into the metalation behavior of porphyrins on oxide surfaces and pave the way for porphyrins metalation on other oxide surfaces and with other metals.

This work is supported by the National Natural Science Foundation of China (Grant No. 21173200), National Basic Research Program of China (2010CB923302, 2013CB834605) and the Specialized Research Fund for the Doctoral Program of Higher Education (SRFDP) of Ministry of Education (Grant No. 20113402110029). J.M.G. thanks the Chinese Academy of Sciences for a Visiting Professorship for Senior International Scientists (Grant No. 2011T2J33) and the German Science Foundation (DFG) for support through the Collaborative Research Centre I083.

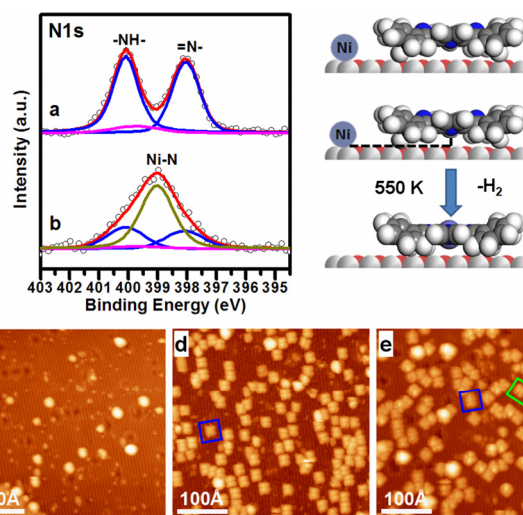


Figure 4. N 1s XP spectra of (a) 2HTPP monolayer on pre-deposited Ni on  $\text{TiO}_2(110)-1 \times 1$  at 300 K ( $\theta_{\text{Ni}} = 0.0985$ ). (b) after heating the sample to 550 K. Constant-current STM images of (c) Ni on  $\text{TiO}_2(110)$  ( $\theta_{\text{Ni}} = 0.01$ ); (d) after deposition of 2HTPP on Ni/ $\text{TiO}_2(110)$  at 300 K (Ni:2HTPP = 1:1); (e) after subsequent heating sample (d) to 550 K. Tunnelling parameters: (c)  $I = 0.03$  nA; (d)  $I = 0.06$  nA; (e)  $I = 0.03$  nA; in all cases  $U = -2.2$  V.

## Notes and references

<sup>a</sup>National Synchrotron Radiation Laboratory and Collaborative Innovation Center of Suzhou Nano Science and Technology, University of Science and Technology of China, Hefei, 230029, P. R. China, jfzhu@ustc.edu.cn.

<sup>b</sup>Fachbereich Chemie, Philipps-Universität Marburg, Hans-Meerwein-St., 35032 Marburg, Germany, michael.gottfried@chemie.uni-marburg.de.

Electronic Supplementary Information (ESI) available: See DOI:

- (a) I. Beletskaya, V. S. Tyurin, A. Y. Tsvadze, R. Guillard and C. Stern, *Chem. Rev.*, 2009, **109**, 1659; (b) D. Bonifazi, A. Kiebele, M. Stöhr, F. Cheng, T. Jung, F. Diederich and H. Spillmann, *Adv. Funct. Mater.*, 2007, **17**, 1051.
- (a) J. Kim, S.-H. Lim, Y. Yoon, T. D. Thangadurai and S. Yoon, *Tetrahedron Lett.*, 2011, **52**, 2645; (b) D. P. Arnold, D. Manno, G. Micocci, A. Serra, A. Tepore and L. Valli, *Thin Solid Films*, 1998, **327**, 341; (c) L. Wang, H. Li, J. Deng and D. Cao, *Curr. Org. Chem.*, 2013, **17**, 3078; (d) A. Tepore, A. Serra, D. Manno, L. Valli, G. Micocci and D. P. Arnold, *J. Appl. Phys.*, 1998, **84**, 1416.
- C. Waeckerlin, K. Tarafder, D. Siewert, J. Girovsky, T. Haehlen, C. Iacovita, A. Kleibert, F. Nolting, T. A. Jung, P. M. Oppeneer and N. Ballav, *Chem. Sci.*, 2012, **3**, 3154.
- I. Mochida, K. Suetsugu, H. Fujitsu and K. Takeshita, *J. Phys. Chem.*, 1983, **87**, 1524.
- (a) W. Auwärter, A. Weber-Bargioni, S. Brink, A. Riemann, A. Schiffrin, M. Ruben and J. V. Barth, *ChemPhysChem*, 2007, **8**, 250; (b) F. Buchner, K. Flechtner, Y. Bai, E. Zillner, I. Kellner, H.-P. Steinrück, H. Marbach and J. M. Gottfried, *J. Phys. Chem. C*, 2008, **112**, 15458; (c) F. Buchner, K.-G. Warnick, T. Wölfle, A. Görling, H.-P. Steinrück, W. Hieringer and H. Marbach, *J. Phys. Chem. C*, 2009, **113**, 16450; (d) F. Buchner, V. Schwald, K. Comanici, H.-P. Steinrück and H. Marbach, *ChemPhysChem*, 2007, **8**, 241; (e) D. Ćcija, W. Auwärter, S. Vijayaraghavan, K. Seufert, F. Bischoff, K. Tashiro and J. V. Barth, *Angew. Chem., Int. Ed.*, 2011, **50**, 3872; (f) K. Flechtner, A.

- Kretschmann, L. R. Bradshaw, M.-M. Walz, H.-P. Steinrück and J. M. Gottfried, *J. Phys. Chem. C*, 2007, **111**, 5821; (g) A. Kretschmann, M.-M. Walz, K. Flechtner, H.-P. Steinrück and J. M. Gottfried, *Chem. Commun.*, 2007, 568; (h) T. E. Shubina, H. Marbach, K. Flechtner, A. Kretschmann, N. Jux, F. Buchner, H.-P. Steinrück, T. Clark and J. M. Gottfried, *J. Am. Chem. Soc.*, 2007, **129**, 9476; (i) A. Weber-Bargioni, J. Reichert, A. P. Seitsonen, W. Auwärter, A. Schiffrin and J. V. Barth, *J. Phys. Chem. C*, 2008, **112**, 3453; (j) J. M. Gottfried, K. Flechtner, A. Kretschmann, T. Lukaszczuk and H.-P. Steinrück, *J. Am. Chem. Soc.*, 2006, **128**, 5644.
- 6 (a) M. Chen, X. Feng, L. Zhang, H. Ju, Q. Xu, J. Zhu, J. M. Gottfried, K. Ibrahim, H. Qian and J. Wang, *J. Phys. Chem. C*, 2010, **114**, 9908; (b) F. Buchner, I. Kellner, H.-P. Steinrück and H. Marbach, *Z. Phys. Chem.*, 2009, **223**, 131.
- 7 (a) K. Diller, F. Klappenberger, M. Marschall, K. Hermann, A. Nefedov, C. Wöll and J. V. Barth, *J. Chem. Phys.*, 2012, **136**, 014705; (b) S. Ditze, M. Stark, M. Drost, F. Buchner, H.-P. Steinrück and H. Marbach, *Angew. Chem., Int. Ed.*, 2012, **51**, 10898; (c) A. Goldoni, C. A. Pignedoli, G. Di Santo, C. Castellarin-Cudia, E. Magnano, F. Bondino, A. Verdini and D. Passerone, *ACS Nano*, 2012, **6**, 10800; (d) M. Stark, S. Ditze, M. Drost, F. Buchner, H.-P. Steinrück and H. Marbach, *Langmuir*, 2013, **29**, 4104; (e) J. Nowakowski, C. Wäckerlin, J. Girovsky, D. Siewert, T. A. Jung and N. Ballav, *Chem. Commun.*, 2013, **49**, 2347; (f) J. Xiao, S. Ditze, M. Chen, F. Buchner, M. Stark, M. Drost, H.-P. Steinrück, J. M. Gottfried and H. Marbach, *J. Phys. Chem. C*, 2012, **116**, 12275.
- 8 (a) I. Mochida, K. Tsuji, K. Suetsugu, H. Fujitsu and K. Takeshita, *J. Phys. Chem.*, 1980, **84**, 3159; (b) I. Mochida, K. Suetsugu, H. Fujitsu, K. Takeshita, K. Tsuji, Y. Sagara and A. Ohyoshi, *J. Catal.*, 1982, **77**, 519.
- 9 (a) J. Niu, B. Yao, Y. Chen, C. Peng, X. Yu, J. Zhang and G. Bai, *Appl. Surf. Sci.*, 2013, **271**, 39; (b) D. Chen, D. Yang, J. Geng, J. Zhu and Z. Jiang, *Appl. Surf. Sci.*, 2008, **255**, 2879.
- 10 A. Rienzo, L. C. Mayor, G. Magnano, C. J. Satterley, E. Ataman, J. Schnadt, K. Schulte and J. N. O'Shea, *J. Chem. Phys.*, 2010, **132**, 084703.
- 11 M. Lackinger, M. S. Janson and W. Ho, *J. Chem. Phys.*, 2012, **137**, 234707.
- 12 W. Auwärter, F. Klappenberger, A. Weber-Bargioni, A. Schiffrin, T. Strunskus, C. Wöll, Y. Penne, A. Riemann and J. V. Barth, *J. Am. Chem. Soc.*, 2007, **129**, 11279.
- 13 (a) F. Buchner, J. Xiao, E. Zillner, M. Chen, M. Röckert, S. Ditze, M. Stark, H.-P. Steinrück, J. M. Gottfried and H. Marbach, *J. Phys. Chem. C*, 2011, **115**, 24172; (b) F. Buchner, E. Zillner, M. Röckert, S. Gläbel, H.-P. Steinrück and H. Marbach, *Chem.-Eur. J.*, 2011, **17**, 10226.
- 14 (a) T. Minato, Y. Sainoo, Y. Kim, H. S. Kato, K.-i. Aika, M. Kawai, J. Zhao, H. Petek, T. Huang, W. He, B. Wang, Z. Wang, Y. Zhao, J. Yang and J. G. Hou, *J. Chem. Phys.*, 2009, **130**, 124502. (b) U. Diebold, *Surf. Sci. Rep.*, 2003, **48**, 53.
- 15 J. Zhou, Y. C. Kang and D. A. Chen, *Surf. Sci.*, 2003, **537**, L429.
- 16 S. Vijayaraghavan, Supramolecular architectures as templates for atomic and molecular confinement. *Dissertation*, Technical University Munich, Munich, 2013.